Load transfer model for piles in calcareous soil

Modèle de transfert de charge pour les pieux dans les sols calcaires

M.F.RANDOLPH, The University of Western Australia, Australia
R.J.JEWELL, The University of Western Australia, Australia

SYNOPSIS: The design of pile foundations to support offshore oil and gas production platforms has generally focused on the peak load that the piles must withstand, treating that load as a single (static) event. However, in calcareous deposits, more attention must be paid to the cyclic nature of loading on offshore platforms. Laboratory and field tests have shown that the axial pile response deteriorates under cyclic loading at load levels well below the static capacity. A model of the load transfer response along the shaft of piles installed in calcareous deposits, with particular emphasis on modelling the degradation under cyclic loading, has been implemented in a computer code, RATZ. The model has been used to match experimental data and to assess the likely response of prototype piles. The paper outlines the principal features of the load transfer model, and discusses the main assumptions incorporated in the model. Comparisons with experimental data are presented and a typical prototype situation is analysed and used to provide guidelines for the design of piles in calcareous soil.

1 INTRODUCTION

In many soil types, the axial capacity of a pile reduces under the action of cyclic loading. This is particularly true with calcareous soils and with loose silica sands, where compressive volume strains in the soil around the pile can lead to a reduction in the normal effective stress acting on the pile, and thence to a reduction in the available skin friction. In such cases, it is important to consider the cumulative effect of cyclic loading over the design life of the pile foundation, and to assess the degree of degradation in capacity. Clearly, the pile capacity must not drop below the peak design load, factored appropriately to allow for uncertainties in the estimated load and in the assumed material response.

The design of pile foundations in calcareous sediments has been discussed extensively in the proceedings of the recent international conference (Jewell and Andrews, 1988). The low axial capacity of driven piles in this material has led to a preference for drilled and grouted piles, where steel tubulars are lowered into a pre-bored hole and the annular gap filled with cement grout. In this way, the pile is effectively bonded to undisturbed soil, taking advantage of any natural cementation present in the soil. Under monotonic loading, the peak skin friction will depend both on the degree of cementation in the soil, and also on the effective radial stress acting on the pile shaft (Randolph, 1988). Initially, the radial effective stress will be that re-established during the grouting process. However, subsequent stress changes will occur during monotonic and cyclic loading, which will affect the ultimate axial capacity of the pile.

Analysis of the axial response of offshore piles is generally accomplished by means of load transfer analysis (Coyle and Reese, 1966), where the soil interaction with the pile (considered as an elastic bar) is modelled as a number of independent, non-linear, springs along the pile shaft. The response of each spring is represented by a load transfer curve, giving the shear stress as a function of the local pile displacement. In order to analyse the pile response under cyclic loading, the load transfer curves must be modified to allow for degradation in skin friction under monotonic and cyclic loading.

This paper describes the development of load transfer models for piles in calcareous soil, with particular attention being paid to the manner in which cyclic loading may be modelled. The load transfer models have been incorporated into a computer code, RATZ, for the analysis of prototype piles to assess the effects of design load sequences. The principal features of the load transfer model are described, and example applications are presented based on experimental data and a hypothetical prototype pile situation.

2 CHARACTERISTIC LOAD TRANSFER RESPONSE

Before describing the load transfer model, the main features of the shearing response of piles in calcareous soil are discussed, in the light of laboratory and field test data. In the laboratory, drilled and grouted piles may be modelled by grouting small diameter rods into pre-drilled holes in soil samples. Such tests are generally referred to as rod shear tests. The test may be conveniently performed in standard soil samples of 70 - 100 mm in diameter, using rods of 10 - 20 mm in diameter. Results of rod shear tests conducted on calcareous soil from the North West Shelf of Australia have been presented by Fahey and Jewell (1988) and by Jewell and Randolph (1988). A typical result from a monotonic loading test is shown here in Figure 1.

Peak skin friction is reached at a displacement that varies with the diameter of the pile (or rod), with a lower limit of 1 - 2 mm. This minimum displacement appears to be associated with that required to form a failure surface in the soil around the pile. In small scale tests, such

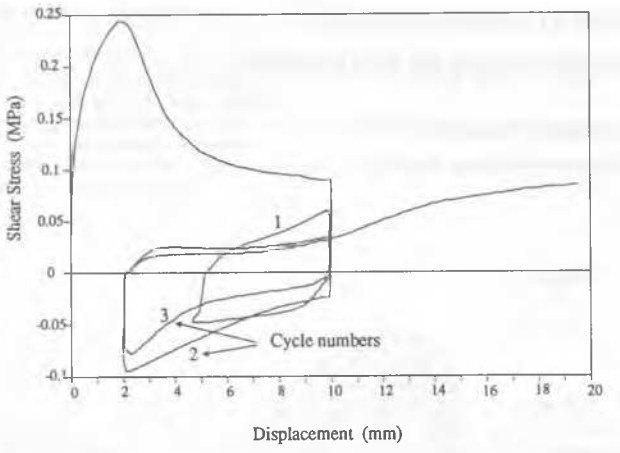

Figure 1. Monotonic rod shear test in calcarenite

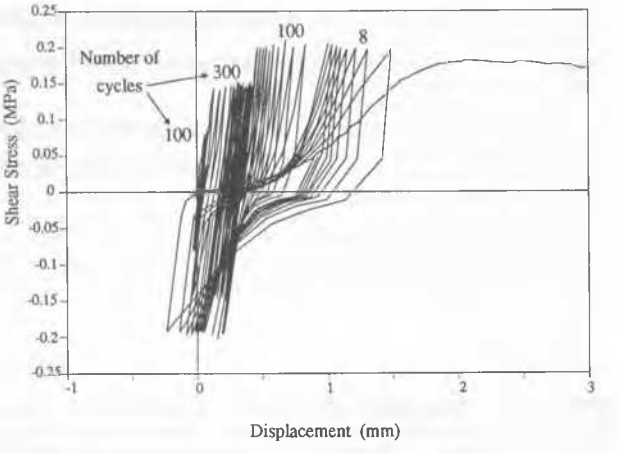

Figure 2. Two-way cyclic rod shear test in calcarenite

local displacement dominates the elastic component which will be typically 0.5 - 1 % of the pile diameter (Randolph, 1988). For prototype piles of diameters 1.5 - 2 m, the elastic component will be much larger relative to the local component, with total displacements to mobilise peak skin friction that are typically in the range 10 - 20 mm (0.5 - 1 % of pile diameter).

The post-peak response shows significant strain softening under monotonic loading. The rate of decrease of skin friction appears to be much more severe in small scale rod shear tests than for tests at field scale (see, for example, Hyden et al (1988)). The decrease in skin friction is due to reducing radial effective stresses acting on the pile, arising from compressive volumetric strains in the highly sheared soil in the failure zone. From cavity expansion theory, the change in radial stress resulting from a given displacement of the cavity wall is inversely proportional to the cavity radius. As such, the change in radial effective stress will be greater for small diameter piles than for large diameter piles (Randolph, 1988), which explains the high rate of strain softening observed in rod shear tests.

An interesting feature of the test shown in Figure 1 is the very low shearing resistance under large displacement cyclic loading. The resistance appears to build up towards the extremities of each cycle, and returns to the original 'monotonic' value during further monotonic shearing. The very low resistance during post-peak cyclic loading may be important in assessing the response of relatively flexible prototype piles, where the upper part of the pile will undergo large displacement cycles during design storm conditions.

A typical rod shear test response during two-way (symmetric) cyclic loading is shown in Figure 2. The numbers of cycles at each shear stress level are indicated on the Figure. At low shear stress levels, the cyclic response is effectively elastic, with a very narrow hysteresis loop. At higher shear stress levels, the hysteresis loop gradually widens, and takes on a pronounced 'S' shape. The shape is consistent with the very low cyclic resistance seen in the large displacement cycles of Figure 1. Eventually, failure occurs after 108 cycles at ± 200 kPa, which is about 60 % of the static skin friction obtained in a test

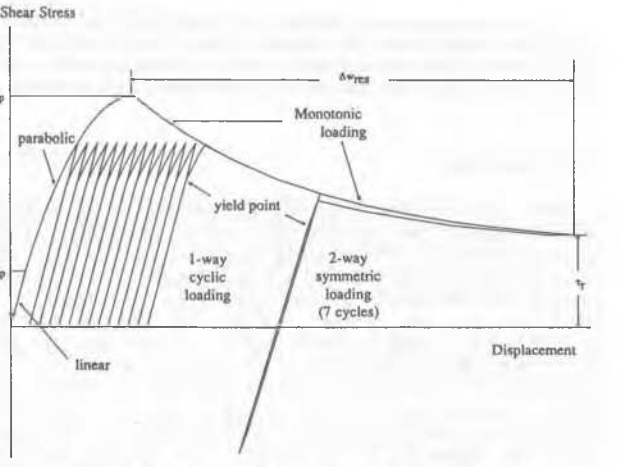

Figure 3. Load transfer curve in RATZ

on a companion sample. It is of interest to note in Figure 2 that, although the loading is symmetric, the pattern of accumulated displacement shows a bias towards positive displacements. It was found that in most two-way (symmetric) cyclic loading tests, some bias was found in the displacement response, although the direction of bias varied from test to test.

3 LOAD TRANSFER MODEL

3.1 Monotonic loading

A general form of load transfer curve for axial pile analysis has been described by Randolph (1986). The curve is shown in Figure 3. Under monotonic loading, the curve consists of three parts:

(1) an initial linear part up to a shear stress of $\xi\tau_p$, where τ_p is the peak skin friction and ξ is a parameter between 0 and 1;

(2) a non-linear part, taken as parabolic in shape, up to the peak skin friction of τ_p;

(3) a strain softening part to a residual value

of skin friction reached at an additional displacement Δw_{res}.

The initial gradient of the load transfer curve is obtained from the elastic shear modulus (G) of the soil, making use of the solution for axially loaded piles presented by Randolph and Wroth (1978), whereby the gradient k is given by

$$k = \frac{d\tau}{dw} = \frac{G}{\zeta r_o} \qquad (1)$$

Here, r_o is the radius of the pile and the parameter ζ depends on the slenderness ratio of the pile but is typically about 4 for a prototype offshore pile.

The form of the strain softening part of the curve is expressed as

$$\tau_f = \tau_p - 1.1(\tau_p - \tau_r)[1 - \exp\{-2.4(\frac{\Delta w}{\Delta w_{res}})^{\eta}\}] \qquad (2)$$

where τ_f is the current skin friction and η is a parameter to adjust the shape of the strain softening curve, generally in the range 0.5 - 1.5.

3.2 Cyclic loading

Of crucial importance to the analysis of offshore piles is the manner in which cyclic loading is modelled. It is assumed that the failure shear stress on reverse loading is identical to the current value for forward loading. However, as can be seen in Figure 3, the response during cyclic loading is taken as linear up to a yield point, after which the response resumes the original parabolic shape. The difference in displacement between the parabolic shape and a purely linear response is considered as 'plastic' displacement, and results in degradation of skin friction in an identical manner to post-peak displacements (see equation (2)).

Figure 3 shows the response under two different forms of cyclic loading. Under purely one-way loading, each cycle consists of an elastic unloading to τ_{min}, followed by a partly linear (elastic) and partly parabolic loading portion, which gives rise to incremental displacement as described above. Since the incremental displacement gives rise to degradation of skin friction, failure will ultimately occur when sufficient displacement has accumulated to rejoin the monotonic loading curve, as seen in the Figure.

Under loading which causes yielding in the reverse direction as well as in the forward direction (for example, symmetric two-way loading), 'plastic' displacement occurs even though there may be no net accumulation of displacement. For each cycle, the plastic displacement used to assess the degree of degradation is just twice the width of the hysteresis loop. If sufficient cycles are conducted such that the skin friction degrades to below the maximum applied shear stress, then failure may occur. This is shown in Figure 3, where 7 cycles of symmetric two-way loading (lying over the top of each other) lead to sufficient plastic displacement to cause failure.

Clearly, the amount of degradation which occurs under cyclic loading is critically affected by the choice of 'yield' point on reloading. The yield shear stress, τ_y, is written in terms of the (algebraic) minimum shear stress τ_{min} and the current failure shear stress τ_f as

$$\tau_y = \tau_{min} + 0.5(1 + \xi)(\tau_f - \tau_{min}) \qquad (3)$$

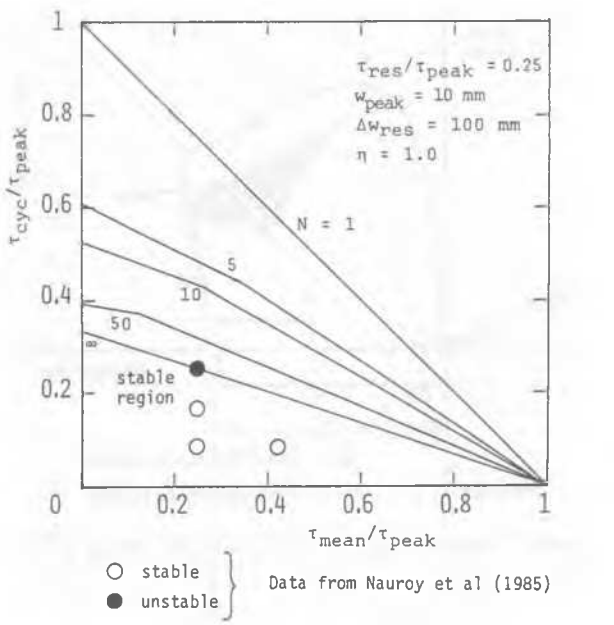

Figure 4. Interaction diagram showing contours of number of cycles to failure

The parameter ξ thus controls not only the degree of non-linearity of the initial loading curve, but also the response under cyclic loading. For $\xi = 1$, the initial response is linear right up to failure, and under cyclic loading the yield point is equal to the current skin friction (giving no degradation unless the current skin friction is mobilised). For $\xi = 0$, the initial loading curve is entirely parabolic, and the yield point is given by

$$\tau_y = 0.5(\tau_f + \tau_{min}) \qquad (4)$$

For one-way loading with τ_{min} equal to zero, the yield point is half the current failure shear stress, while for symmetric two-way loading, the yield point may be calculated as one third of the failure stress (since $\tau_{min} = -\tau_y = -\tau_f/3$). For cyclic shear stress values in excess of these limits, incremental plastic displacement will occur with each cycle, leading ultimately to failure (provided the residual skin friction is low enough).

The elastic thresholds implied by equation (4) are identical to those originally suggested by Goodman in relation to fatigue of metals (for example, Moore and Kommers (1927)), where the fatigue thresholds for one-way and symmetric two-way loading were taken respectively as one half and one third of the ultimate tensile strength of the metal.

Rather than plot cyclic failure limits on a traditional Goodman diagram (as in fatigue analysis of metals), it is more common in geotechnical work to consider an interaction diagram with the normalised cyclic shear stress amplitude, τ_c/τ_p, plotted against the normalised mean shear stress, τ_m/τ_p. Such a diagram is shown in Figure 4, showing contours of the number of cycles, N, to failure. While the straight line limits for N = 1 and N = ∞ are independent of the precise form of the load transfer curve (assuming $\xi = 0$), the position of the other contours will

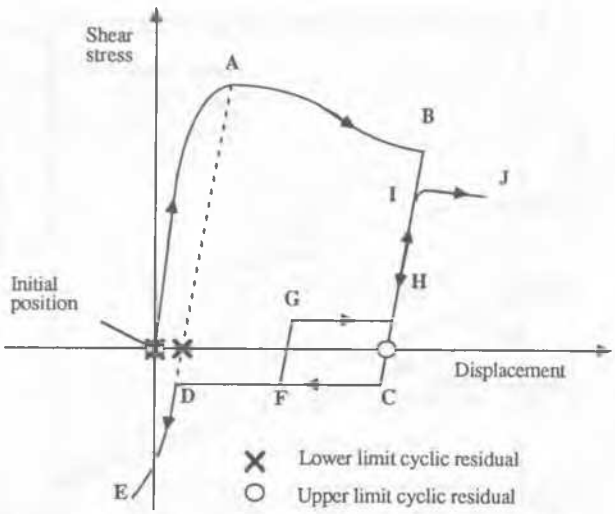

Figure 5. Modelling cyclic residual shear stress

depend on the value of parameters such as η, and the ratio of the displacement at peak skin friction to the additional displacement to residual. The data points shown on the Figure are discussed later in the paper.

3.3 Cyclic residual

There is one further aspect of the cyclic response of calcareous soil which needs to be considered, and that is the very low resistance seen over the central region of post-peak large displacement cycles (Figure 1) or pre-peak cycles close to failure (Figure 2). The observed response has been modelled as shown schematically in Figure 5. Two markers are used to indicate the extent of a zone within which the shear resistance is limited to a 'cyclic residual' value.

Initially, the two markers are positioned together at the origin of the load transfer curve. Before failure the two markers move together, staying at the point where an elastic unloading line cuts the displacement axis. After failure, whether brought about by pre-peak cyclic loading or by monotonic loading to point A, the upper limit marker (the circle in Figure 5) continues to track the current position of the shear stress displacement point, while the lower limit marker (the cross) stays fixed. On unloading, the path BCDE is followed, with the shear resistance staying at the cyclic residual value from C to D. If the element is reloaded, from point F, the shear resistance remains at the cyclic residual value until the upper marker is reached, following the path FGHIJ. The shear resistance at point I will be lower than at point B, due to the additional plastic displacement undergone.

4 EXAMPLE APPLICATIONS

The load transfer model described above has been incorporated into a computer program, RATZ (Randolph (1986)). The program is used here in two examples which illustrate the effects of cyclic loading for piles embedded in calcareous soil.

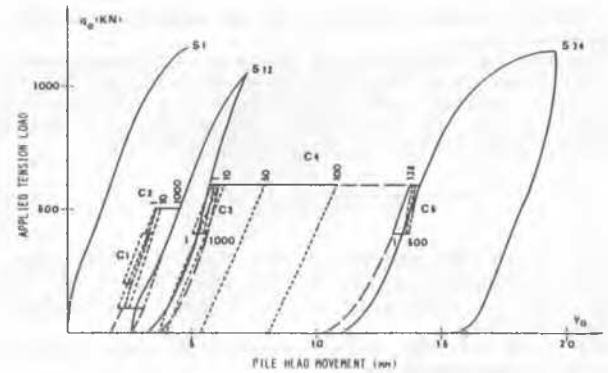

Figure 6. Results of Plouasne pile load test (Nauroy et al (1985))

Table 1 Cyclic loading packets (Nauroy et al (1985))

Load Packet	Average Load (kN)	Cyclic Load (kN)	Number of cycles
C_1	300	100	1000
C_2	300	200	1000
C_3	500	100	1000
C_4	300	300	138
C_5	500	100	500

The first example is from a field scale pile test in calcareous soil in France, while the second is a hypothetical design situation, based on calcareous soil properties typical of the North West Shelf of Australia.

4.1 Plouasne pile (Nauroy et al (1985))

Nauroy et al (1985) report the results of monotonic and cyclic loading tests performed on a drilled and grouted pile at Plouasne in France. The pile consisted of a steel tube of external diameter 0.22 m, and wall thickness 10 mm, grouted into calcareous sand between depths of 7.5 and 14.5 m. Nauroy et al (1988) quote final measured dimensions of the pile of 7 m long by 0.35 m average diameter, giving a surface area of 7.7 m^2.

Monotonic loading tests gave an initial capacity of the pile of about 1200 kN (average skin friction of 156 kN), decreasing to about 500 kN (65 kPa) after a displacement of 200 mm. The pile head stiffness varies between about 250 and 400 kN/mm, depending on the load range. The measured response under various packets of cyclic loading is shown in Figure 6 (from Nauroy et al, 1985). Table 1 gives details of each loading packet. The measured pile response shows that only packets C4 (138 cycles of load, 300 ± 300 kN) and, to a lesser extent C2 (1000 cycles of load, 300 ± 200 kN) give rise to appreciable displacement of the pile head. The load packets are plotted on Figure 4, in terms of average applied shear stress normalised by the average shear stress at failure of 156 kPa (pile capacity of 1200 kN). It is interesting to note that load packet C_4 is the only one which falls on the boundary of the stable region below the contour for N = ∞.

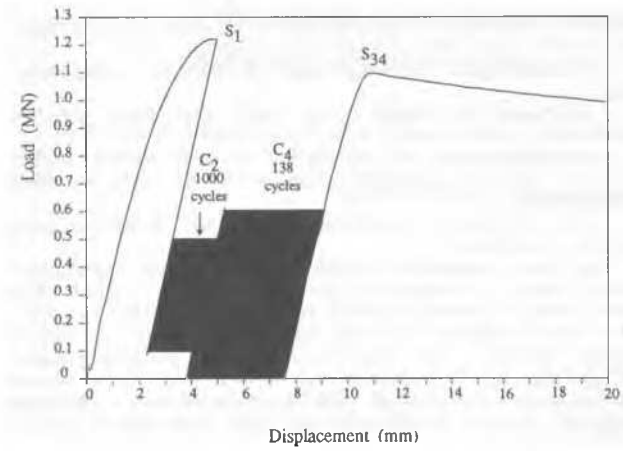

Figure 7. Numerical results for Plouasne test

In modelling the pile response, values of elastic shear modulus, G, and peak skin friction, τ_p, have been taken as approximately proportional to depth (as might be expected for a silica sand for that depth range). This assumption is consistent with the largely uncemented nature of the calcareous sand at Plouasne. In order to match the pile stiffness and peak capacity, the elastic shear modulus has been taken as G = 50 MPa at the top of the pile, increasing to 100 MPa at the pile tip, while the peak skin friction has been assumed to vary from 110 kPa to 220 kPa over the 7 m interval. These values give a peak pile capacity of 1200 kN, mobilised at a pile head displacement of just under 5 mm.

Figure 7 shows the pile response computed using the program, RATZ, for the loading sequence shown in Figure 6 (omitting the static test S_{12}). The load packets C_1, C_3 and C_5 were found to yield elastic response of the pile (within the assumptions of the load transfer model), and so are not evident on the Figure. Incremental displacements during the other two load packets are 1.7 mm for C_2 (compared with about 1 mm actually measured) and 4 mm for C_4 (compared with 8 mm actually measured). Thus although the field measurements are not matched precisely, the general trend is well represented. The static loading at the end of cyclic loading gave a reduced capacity of 1100 kN, which agrees with that reported by Nauroy et al (1985).

4.2 Offshore drilled and grouted pile

The predicted response of an offshore drilled and grouted pile during a design storm is discussed below. The pile has been taken as a steel pipe, 1.7 m in diameter by 50 mm wall thickness, grouted into a 50 m long by 2 m diameter hole. For simplicity, uniform soil properties have been taken, as given in Table 2.

The assumed storm loading sequence (based on factored loads) is given in Table 3. The peak load ($P_{mean} + P_{cyclic}$) of 65 MN compares with an ideal pile capacity (assuming a rigid pile) of 94 MN and an actual static capacity (allowing for strain softening) of 87 MN.

The response to the storm loading is shown in Figures 8(a) and (b). At the end of the storm loading, the static capacity of the pile has been

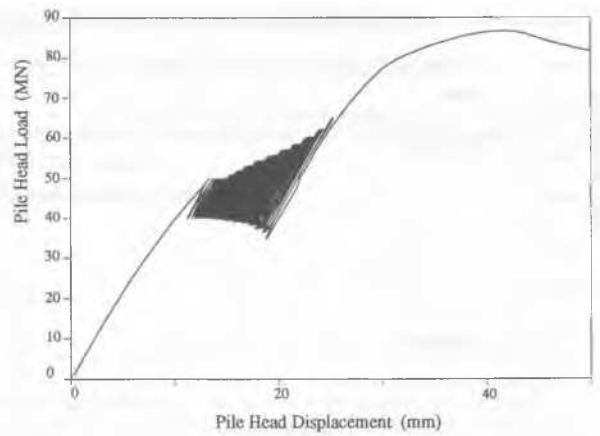

(a) Pile head load against displacement

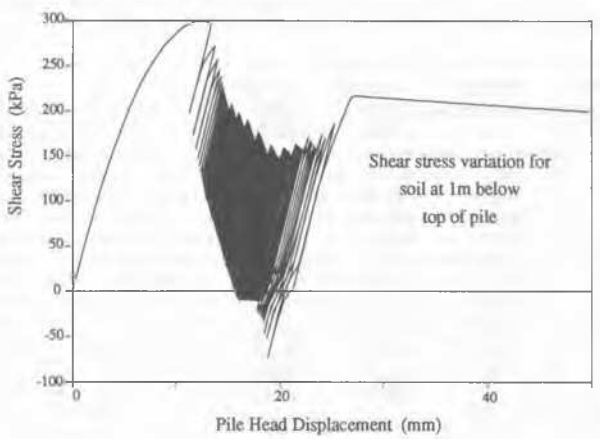

(b) Shear stress against displacement

Figure 8. Offshore pile under storm loading

Table 2 Load transfer parameters

Shear modulus G (MPa)	200
Parameter ζ	4
Yield parameter ξ	0
Peak skin friction τ_p (kPa)	300
Res. skin friction τ_r (kPa)	30
Cyc. res. shear stress τ_{cr} (kPa)	10
Displacement to residual Δ_{res} (mm)	1000
Strain softening parameter η	0.7

reduced only marginally, to 86 MN. The shear stress response of the upper soil element (1 m below the top of the pile) shows that the element reaches its peak skin friction during the initial loading of the pile. This creates a 'gap' under cyclic loading (in the manner of Figure 5) of just under 2 mm. During the subsequent cyclic loading, the mean shear stress at the upper soil element gradually reduces, due to yielding of the element under each cycle. In fact, the pile shakes down to a purely elastic response under the first five packets of loading. In the later load packets, the effect of the low cyclic res-

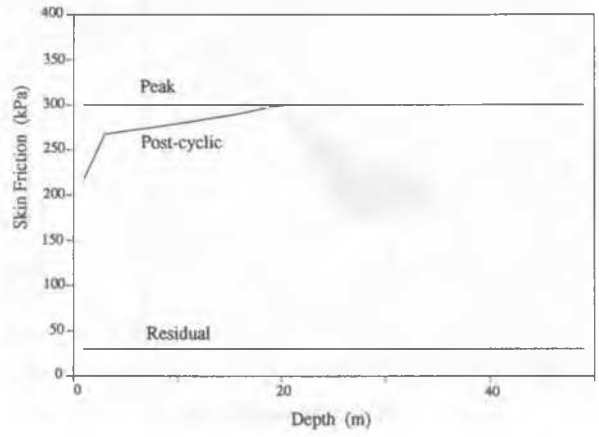

Figure 9. Profiles of skin friction down pile

Table 3 Storm loading pattern (factored loads)

Wave Height (m)	Number of cycles	Average Load (MN)	Cyclic Load (MN)
10	500	45.0	5.0
11	300	45.5	5.5
12	180	46.0	6.0
13	100	46.5	6.7
14	50	47.0	7.5
15	30	47.5	8.3
16	15	48.0	9.2
17	8	48.5	10.2
18	5	49.0	11.5
19	2	49.5	13.0
20	1	50.0	15.0

idual shear stress may be seen, whereby the negative shear stress is initially limited to the cyclic residual value. Only when the displacement amplitude becomes large enough for the element to be displaced beyond the gap width (as in path FDE in Figure 5) does the negative shear stress start to exceed the cyclic residual value. The 'S' shape response observed in element tests (for example, Figure 2) may be clearly seen in the latter load cycles.

One of the key questions facing the engineer in offshore pile design is the extent to which a given loading sequence may degrade the soil at any particular depth. This may be illustrated by plotting profiles of skin friction (initial peak, current and residual) at the end of a given load sequence. Figure 9 shows such a profile at the end of the storm loading (before the final static loading). It may be seen that some degradation in skin friction is observed over the upper 20 m of the pile, even though the static capacity has been hardly affected.

5 CONCLUSIONS

This paper has presented a model for the axial load transfer of piles in calcareous soil. The model is phenomenological in nature, based on observations of the response of laboratory and field element element tests to montonic and cyclic loading. Key features of the load transfer model are the ability to model:

- degradation under large monotonic displacement;
- degradation under pre- and post-peak cyclic loading;
- accumulation of permanent displacement under biased cyclic loading (subject to an assumed threshold);
- low cyclic resistance during post-failure cyclic loading.

The load transfer algorithm has been incorporated into a computer program, RATZ, which has been used to model field pile tests, and to predict the response of typical offshore piles under storm loading. At this stage, the pile response predicted by the numerical model has been shown to be consistent with field experiments, lending support to the usefulness of the approach in offshore pile design.

Further development and calibration of the load transfer model is currently being conducted at the University of Western Australia. In particular, the effect of pile diameter on peak and residual values of skin friction and on the post-peak shape of the load transfer curve is being explored. Results from field scale pile load tests which demonstrate such diameter effects are being simulated through finite element analysis incorporating a numerical model of calcareous soil. This work will provide a framework whereby load transfer curves established from laboratory scale model pile tests and rod shear tests may be extrapolated with greater confidence for the design of prototype drilled and grouted piles.

REFERENCES

Coyle H.M. & L.C.Reese 1966. Load transfer for axially loaded piles in clay, J. Soil Mech. and Found. Eng., ASCE, 92(SM2), 1-26.

Hyden A.M., J.M.Hulett, J.D.Murff & A.F.Abbs 1988. Design practice for grouted piles in Bass Strait calcareous soils, Proc. Int. Conf. on Calcareous Sediments, Perth, 2, 297-304.

Jewell R.J. & D.C.Andrews (Eds.) 1988. Engineering for Calcareous Sediments: Proc. Int. Conf. on Calcareous Sediments, Perth, Volumes 1 & 2.

Jewell R.J. & M.F.Randolph 1988. Cyclic rod shear tests in calcareous sediments, Proc. Int. Conf. on Calcareous Sediments, Perth, 2, 215-222.

Moore H.F. & J.B.Kommers 1927. The Fatigue of Metals, McGraw-Hill, New York.

Nauroy J-F., F.Brucy & P.Le Tirant 1985. Static and cyclic load tests on a drilled and grouted pile in calcareous sands, Proc. Int. Conf. on the Behaviour of Offshore Structures, BOSS'85, Delft.

Nauroy J-F., F.Brucy & P.Le Tirant 1988. Skin friction of piles in calcareous soil, Proc. Int. Conf. on Calcareous Sediments, Perth, 2, 239-244.

Randolph M.F. 1986. RATZ: Load transfer analysis of axially loaded piles, Report Geo:86033, Department of Civil Engineering, The University of Western Australia.

Randolph M.F. 1988. The axial capacity of deep foundations in calcareous soil, Proc. Int. Conf. on Calcareous Sediments, 2, Perth.

Randolph M.F. & C.P.Wroth 1978. Analysis of deformation of vertically loaded piles, J. Geot. Eng. Div., ASCE, 104(GT12), 1465-1488.